Radio Emission from Supernova Remnants 77

Gloria Dubner

Abstract

Supernova remnants (SNRs) can radiate their energy across the whole electromagnetic spectrum, but they are principally radio emitters, and investigations in the radio range have provided deep insight into the properties, the evolutionary characteristics, and the physical processes at play. Radio observations permit to delimit the current location of the expanding shock front, to identify sites of particle acceleration, to infer orientation and degree of order of compressed magnetic fields, and to investigate the coupling between the magnetized relativistic wind of the central neutron star and the surrounding plasma. Also, radio observations are a powerful tool to discover new SNRs in our galaxy and in neighboring galaxies. This chapter presents a brief overview of the nature of the radio emission, describing the observable properties that help to constrain theories, i.e., brightness distribution, spectrum, and polarization. The total energy content in a radio remnant is also discussed. In this context, the different morphologies observed in radio remnants and their physical meaning are analyzed. Finally, the problem of linking an SNR with its precursor star and the role of present and future large radio telescopes in the knowledge of SNRs are examined.

Contents

G. Dubner (✉)
Institute of Astronomy and Space Physics (IAFE), CONICET, University of Buenos Aires, Buenos Aires, Argentina
e-mail: gdubner@iafe.uba.ar; gdubner@gmail.com

A.W. Alsabti, P. Murdin (eds.), *Handbook of Supernovae*,
https://doi.org/10.1007/978-3-319-21846-5_91

1 Introduction

Radio waves are the spectral range in which SNRs are more consistently identified. Green's (2014) catalogue shows that about 95 % of the SNRs discovered in our galaxy are radio sources. Only 20 out of 294 remnants identified up to now have not yet been detected in radio or are poorly defined by current radio studies. A galactic radio source with some extension (no point-like), a power law (synchrotron) spectrum, and some linear polarization is almost certainly an SNR.

Radio astronomy played a crucial role in the investigation of supernova remnants (SNRs) both for the discovery of new sources and for a better comprehension of their properties. Before the advent of radio telescopes, only two SNRs were known based on their optical emission, the Crab Nebula and the remnant of Kepler's SN. In 1948, the early years of radio astronomy, using a radio version of Michelson's interferometer, Ryle & Smith detected an exceptionally bright radio source. It turned out that the radiation came from Cassiopeia A, the brightest extrasolar radio source in the sky. In 1949, the radio detection of the Crab Nebula was reported, followed in 1952 by the discovery in radio of the remnant of Tycho's SN and in 1957 of Kepler's SN.

From these early radio studies, two important conclusions were drawn: that the remnant of a supernova is a source of intense radio radiation and that it would be difficult to interpret the observed radiation in terms of strictly thermal processes, as it was early proposed to explain the optical emission of the Crab Nebula. In effect, the suggestion that the observed emission was the result of excitation from an exceptionally hot star (namely, the supernova) or other alternatives proposed by that time, as the radioactive decay of some unstable isotopes produced during the explosion, would require impossibly high temperatures and densities to fit the radio observations.

As the detected emission had nothing in common with thermal black body radiation, the fundamental question of what was powering these sources was a serious problem to solve. The correct idea was proposed for a slightly different context by Alfvén and Herlofson in 1950. They suggested that "radio stars" would radiate energy when relativistic electrons move through a magnetic field "trapped" around the star, in a way similar to what is observed in large synchrotrons. To account for the total energy emitted by a radio star, they advanced the idea that "the cosmic-ray acceleration close to the star can be supplemented by a Fermi process further out of the trapping field." Slightly later, Kiepenheuer published a more general view of the role of cosmic rays as the source of general galactic radio emission.

In those early years of radio discoveries, Shklovsky raised the questions whether all peculiar nebulae resulting from supernova outbursts are radio sources and whether all galactic discrete sources of "nonequilibrium" radio emission must be regarded as remnants of supernova explosions. Based on previous works, mostly of observations of the Crab Nebula, he proposed a completely new explanation for the radio emission of SNRs. Shklovsky followed the inverse approach of his antecessors, and instead of extrapolating the mechanisms that work for optical radiation to the radio regime, he applied the radio synchrotron mechanism to optical wavelengths and concluded that if the hypothesis of synchrotron nature was correct, the definitive proof would be the detection of polarization in the visible light of the Crab Nebula. The prediction was confirmed by Dombrovsky in 1954, followed later by other works. This proved that the conjecture was correct; the origin of radio radiation in SNRs is a synchrotron mechanism. Although Shklovsky made the wrong assumption that "Crab may be taken as a typical remnant of a supernova explosion," and in the following years it was obvious that there are great differences between the Crab Nebula and the rest of SNRs, the conclusions extracted from an exceptional case served to explain the nature of the radio emission of all SNRs.

In what follows, we summarize the basic properties of the radio emission of SNRs, a description of the physical mechanisms at play including the observable parameters, and the distinguishing features of radio remnants.

1.1 Basic Description of the Synchrotron Radiation from SNRs

A single relativistic electron moving in an external magnetic field (electrons spiraling the B field lines) will emit continuum spectrum radiation, reaching its maximum intensity at a critical frequency:

$$\nu_c = (3eB_\perp/4\pi mc).(E/mc^2)^2 = C_1 B_\perp E^2$$

with $C_1 = 16.08$ when ν is in MHz, B in μG, and E in GeV ($B_\perp$ is the component of the magnetic field perpendicular to the electrons path). For example, an electron with energy of 3 GeV in a field of 10 μG will radiate most of its energy at frequencies near 1.5 GHz, the L-band in radio receivers. An observer will see the relativistic electron radiating into a narrow cone around its instant velocity direction, and the half-angle of the cone is of the order of 1/L, with $L = 1/(1 - v^2/c^2)^{1/2}$, the Lorentz factor.

Actually, relativistic particles are not alone, but in an ensemble, and the synchrotron radiation that an observer detects from a particular volume element of a radio source comes from all the electrons with the same pitch angle. We can assume that the source consists of a volume V containing a tangled magnetic field with average strength B, in which there are electrons with an energy density with power law distribution (as the empirical evidence of the cosmic rays close to the Earth shows) $n(E)\,dE = n_0 E^{-p}\,dE$ between a range of energies $E_1 \leq E \leq E_2$

(to avoid divergences in the extremes). In this case, it can be shown that the emitted radiation has a spectrum

$$\varepsilon_\nu \propto \nu^{-(p-1)/2} = \nu^{-\alpha}$$

with $\alpha = (p-1)/2$ the emission spectral index. The most important result is that a power law distribution of electrons radiates a power law emission spectrum. After carrying out the corresponding calculations, it can be shown that the flux density S (specific intensity) of a synchrotron source with a volume V follows the expression

$$\mathrm{S}(\nu)(\mathrm{Jy}) = 0.017\mathrm{a}(\alpha)\mathrm{V}\,\mathrm{B}^{(\alpha+1)}[6.26\times 10^{18}/\nu(\mathrm{Hz})]^{\alpha} \propto \nu^{-\alpha}$$

where a(α) takes values like 0.283 for a spectral index $\alpha = 0$, 0.103 for $\alpha = 0.5$, or 0.085 for $\alpha = 0.75$, the source volume V in cgs units, and B the magnetic field strength. The flux density S is measured in Jy (1 Jansky $= 10^{-26}$ watt/m^2 Hz).

If the flux density is expressed as a brightness temperature, they are related at radio frequencies by the Rayleigh-Jeans approximation and

$$\mathrm{S} = (2k\mathrm{T}\nu^2)/c^2 = 2k\mathrm{T}/\lambda^2$$

where k is the Boltzmann constant.

The degree of polarization of the emission also depends on the electron power law index and is independent of the frequency. For a uniform magnetic field, the intrinsic degree of linear polarization is given by

$$P = \frac{2\alpha + 2}{2\alpha + \frac{10}{3}}$$

For a synchrotron radio source with a spectral index $\alpha = 0.5$, the fractional polarization can reach a maximum theoretical value of about 70 %, but in practice, as will be shown below, a much lower polarization percentage is usually observed.

1.2 Shocks and Shells

The explosion of an SN represents the sudden injection of about 10^{51} ergs in an almost point-like region of the space. It causes a large increase in the local pressure, and the disturbed region expands, while the released stellar ejecta begin sweeping up the surrounding gas, driving a shock wave into the interstellar medium (ISM) heating it to very high temperatures. The leading edge of this expanding disturbance is called the shock front. A shock is an irreversible pressure-driven disturbance, a nonlinear plasma wave generated by plasma flow that forms a transition layer that separates supersonic flow (upstream, with Mach numbers that initially can be greater than 1000) to subsonic flow (downstream). Thus the shock marks the location of an invisible "wall" where density, temperature, magnetic field strength, and flow

speed dramatically change. Flow crosses the surface of a shock accompanied by compression and dissipation. When there is no plasma flow through the surface and there is a density and temperature jump, but pressure and all other quantities (magnetic field, velocity) are continuous, the "wall" is called contact discontinuity.

The supersonic shock created after the SN explosion continuously slows down over time as it sweeps up the ambient medium, but it can expand for hundreds or thousands of years and over tens of parsecs before its speed falls below the local sound speed. The SN blast wave and swept-up matter constitutes the SNR "shell."

Initially a contact discontinuity separates the ejecta from the shocked ISM. No matter whether an SN blast wave encounters a modified or a relatively undisturbed surrounding medium, the shock begins to decelerate when a mass comparable to the ejected mass has been swept up by the shock and the interior ejecta are decelerated abruptly. As ejecta from the interior pile into the decelerated matter, a reverse shock (inward-facing) is formed and shocks the ejecta. The reverse shock begins life very weak and radiative but rapidly strengthens to velocity jumps of order 1000 km/s producing X-ray-emitting temperatures in the ejecta. Realistically, the contact discontinuity is Rayleigh-Taylor (R-T) unstable (an instability that takes place at the interface between two fluids of different densities, when the lighter fluid pushes the heavier fluid) and rapidly can lose the initial spherical symmetry developing R-T fingers. Meanwhile, the outer shock continues to decelerate until the radiative time scales become comparable to the dynamical time. At this point, the shock becomes effectively isothermal with much higher compression ratios than before. Eventually the shock weakens, and all traces of this huge perturbation disappear and merge with the ISM, after modifying in an irreversible way the physical and chemical properties of an area that can span up to hundreds of pc.

In any case, in the compressed region between the contact discontinuity and the leading shock front, there is thermal gas, relativistic particles, and magnetic field producing a shell of radio synchrotron radiation. The interior, strongly disturbed by the passage of two shocks moving in opposite directions, is mostly a low-density, very-high-temperature bubble that emits in X-rays.

1.3 Particle Acceleration and the Radio Spectrum of Shell-Type SNRs

The basis of all theories to explain acceleration mechanisms in shock waves is that particles can gain energy in collisions with irregularities of the magnetic field. In works published by Bell in 1978, and in another contemporaneous article by Blandford and Ostriker, it was demonstrated that charged particles can be accelerated to high energies in astrophysical shock fronts, resulting in a power law energy spectrum with an index $p \approx 2$ consistent with what is found in different astrophysical contexts. The most efficient process for electrons to gain energy after multiple crossing through a shock wave is called diffusive shock acceleration (DSA), also known as first-order Fermi acceleration process. The fast particles are prevented from streaming away upstream of the shock front by scattering off Alfvén

waves which they themselves generate. Such scattering confines the particles to the region around the shock. In each cross particles can gain energy attaining relativistic speeds.

For energetically unimportant test particles which do not influence the flow structure (the so-called test-particle limit), the following relations can be established:

$$\alpha = \frac{p-1}{2} = \frac{3}{2r-2}$$
$$p = \frac{r+2}{r-1}$$
$$r = \frac{\gamma+1}{\gamma-1+\frac{2}{M^2}} \cong \frac{\gamma+1}{\gamma-1}$$

where α is the synchrotron spectral index, p is the particle energy spectral index, r is the ratio between post- and pre-shock densities, γ is the ratio of post and pre-shock-specific heats, and M is the upstream Mach number. In the case of strong shocks with a compression ratio $r = 4$ (as obtained for the common case of a ratio of specific heats of 5/3 and the shock Mach number $\gg 1$), this mechanism predicts a spectral index $\alpha = 0.5$ for the radio flux density S.

However, observational studies of the global and of the spatial distribution of the radio spectrum of SNRs show departures from the standard theoretical predictions. Less than a quarter of the SNRs identified in our galaxy as members of the shell-type SNRs have the theoretically predicted α. As illustrated in the histogram shown in Fig. 1, indices between $\sim$0.2 and $\sim$0.7 are detected in a considerable number of shell SNRs, defying current theories.

It is very important to understand the spectrum as the synchrotron spectral index traces the distribution of energy among relativistic particle populations and the degree of magnetic field compression. Any variation in the particle acceleration translates in different behavior of the spectral index. In the first-order Fermi model, stronger shocks (larger r) yield flatter indices ($\alpha < 0.5$). Regions with magnetic field enhancement and high efficiency in particle acceleration would have flat spectra,

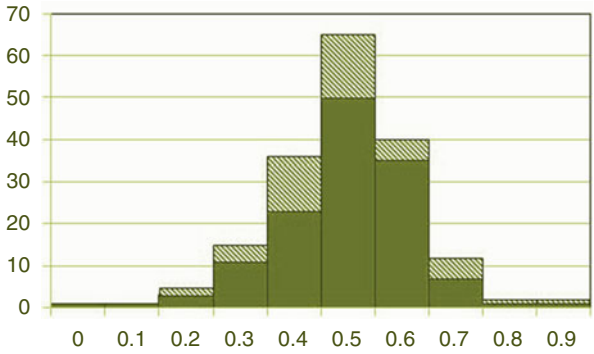

Fig. 1 Histogram of spectral indices of the shell-type SNRs in the Milky Way. The *solid bars* correspond to firmly determined indices, while the *shadowed ones* count sources with uncertain spectral indices, based on data extracted from Green's (2014) catalogue. The histogram is reproduced from Dubner and Giacani (2015)

while steep spectra ($\alpha > 0.5$) are expected in more diffuse emission regions. Sometimes, the global spectrum of SNRs in a logS vs. $\log \nu$ diagram shows a curvature instead of being linear. A curved concave-up spectra (flatter indices at higher frequencies) in young SNRs can be the result of nonlinear DSA effects (the pressure of cosmic ray particles produced at the shock wave has to be included in fluid dynamics equations). While steeper spectra for increasing energy (concave down) can be produced by shocks with low Mach number ($M \leq 10$), although only few SNRs would be expected to have such slow shocks, not enough to explain all the observed cases.

It can also be noticed that theory predicts that the particle acceleration must be very efficient in young SNRs, corresponding to free expansion and especially early Sedov phase of evolution. This effect should translate in flatter spectra (i.e., $\alpha < 0.5$), while steep spectrum is predicted for older remnants, when the shock wave loses energy and particle acceleration is less effective. However, a quick view to the historical shell-type SNRs shows quite the opposite as $\alpha = 0.77$ for Cas A, 0.64 for Kepler's SNR, 0.61 for Tycho's SNR, and 0.60 for SN1006. Moreover, $\alpha \approx 0.8$ for SN 1987A. The explanation for this unexpected behavior was proposed by Bell et al. (2011), who showed that the orientation of the magnetic field has an important role, and young SNRs with a B field oriented quasi-perpendicular to the shock normal should produce steeper spectrum.

In addition, it has to be considered that the shape of the global spectrum can be altered by extrinsic or intrinsic processes that modify the electron energy distribution or the radio propagation between the source and the observer. For example, the low radio frequencies extreme of the spectrum can be affected by thermal absorption, synchrotron self-absorption, and the Tsytovich-Razin effect. Thermal absorption is produced when the nonthermal SNR radiation traverses a region with thermal plasma, producing a low-frequency turnover in the spectrum. Synchrotron self-absorption takes place if the intensity of synchrotron radiation within the source becomes sufficiently high; then reabsorption of the radiation through the synchrotron mechanism may become important. The Tsytovich-Razin effect can only be important in sources with very small size and weak magnetic fields. Figure 2 shows an example of integrated spectrum with a low-frequency turnover probably due to the presence of thermal absorption along the line of sight toward the SNR IC443.

We can ask ourselves if the radio brightness features in SNRs are correlated with specific spectral variations, such as steepening or flattening. The answer is that although in some cases it does, in general it does not. For example, in the young SNR Cas A, the highest emissivity regions tend to be associated with steeper spectral indices, while in the SNRs G39.2–0.3 and G41.1–0.3, spectral variations do not correlate at all with features in total intensity. In older remnants, brighter regions tend to have flatter, but this is not general. Also interaction between the expanding blast wave and the inhomogeneous ambient medium can be an important factor in determining the spatial distribution of spectral indices in shell-type SNRs. In these cases, in general, it is expected to observe flatter indices accompanying the higher Mach number shocks that develop inside the dense cloud.

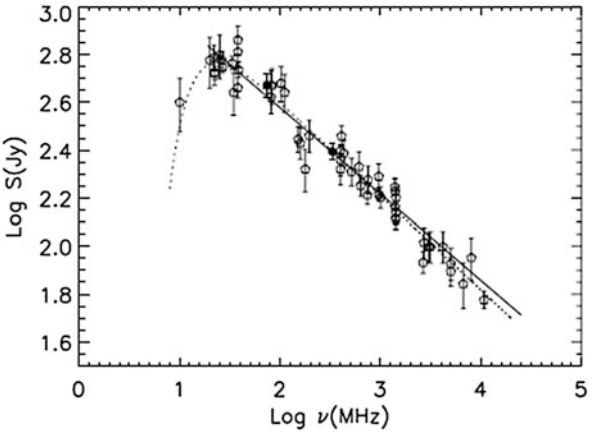

Fig. 2 Radio spectrum of the SNR IC443 showing absorption at low frequencies caused by ionized gas along the *line of sight* (From Castelletti et al. 2011)

In summary, many different factors, both of internal origin (as the efficiency of electron injection or orientation and compression of magnetic field) and of external origin (thermal gas interposed in the line of sight or interaction between the shock wave and surrounding clouds), control the radio spectrum. For extensive discussions and reviews of standard and nonlinear particle acceleration theories, see, for example, Blandford and Eichler (1987), Malkov and O'Drury (2001), Reynolds (2008, 2011), Jones (2011), and Uroševi (2014 and references therein).

1.4 Magnetic Field Origin and Orientation

In 1962, van der Laan suggested that the magnetic field responsible for the synchrotron emission observed in SNRs was the interstellar field compressed by the explosion. The hypothesis was plausible because even a relatively weak compression of the few micro-Gauss of the ambient magnetic field would result in an observable radio source due to the strong dependence of volume emissivity on the magnetic field strength. Van der Laan arrived to the conclusion that even when Shklovsky's theory for nonthermal emission from SNRs was correct in many aspects, it had been developed explicitly for the spherical volume contained by the envelope ejected by the SN explosion (as in the Crab Nebula), and therefore the model was not relevant for the SNRs with a shell-like morphology (i.e., sources where the emission comes from the peripheric shocked gas) that the new radio observations conducted in the late 1950s were revealing. Van der Laan then proposed two different models, both based on the compression of the interstellar medium by an expanding spherical piston composed of ejecta of the SN explosion. The radio emission would be produced between the piston surface and the shock wave preceding the piston in the rims of the shell where the interstellar field has

been compressed. In one of the models, the radiation is due to relativistic electrons from the ISM trapped in the compressed regions. In the other, the flux is due to the injection of relativistic electrons from the SN debris into the compressed volumes. A few years later, Whiteoak and Gardner (1968) provided firm support to this suggestion through a polarization study of the radio SNR G296.5+10.0, a high-latitude source, far from contamination of the galactic plane, where they demonstrated that the magnetic lines were aligned with the expanding shell.

Thus the problem appeared to have been solved, and the compressed interstellar magnetic field was sufficient to produce the radio emission of SNRs. Years later, however, indirect observational arguments, like the thickness of the X-ray rims in the SNRs Cas A, Kepler, Tycho, RCW 86, and SN 1006 and the rapid variability (on timescale of few years) observed in X-ray spots in the SNR RXJ1713.7-3946 and in Cas A, strongly suggested that the magnetic fields must be from tens to hundreds of times more intense than expected from simple adiabatic compression of the interstellar magnetic field, and some extra mechanism of amplification is required.

Several mechanisms were then proposed that result in an amplification of the magnetic field. Cosmic ray streaming can, for example, induce turbulence and instabilities that act to amplify the magnetic field. Some models include amplification due to flow instabilities between the mean flow and clouds in the circumstellar and/or interstellar medium, amplification as a result of very efficient acceleration of nuclear cosmic rays at the outer shock, turbulent amplification driven by cosmic ray pressure, nonlinear diffusive shock acceleration, etc. See, for example, Schure et al. 2012 and Reynolds et al. 2012 reviews on observations and theories for magnetic field amplification in the presence of a cosmic ray population.

However, the global problem about origin, properties, and evolution of the magnetic field in SNRs is still an open question. Radio polarization observations of SNRs provide essential information on the degree of order and orientation of the ordered component of the magnetic field.

The radio radiation in SNRs is expected to be linearly polarized; therefore, from the observed polarization electric vector (the only to which radio telescopes are sensitive), it can, in principle, be determined the direction of the orthogonally aligned magnetic field. Radio telescopes (using feeds sensitive to orthogonal circular or linear polarizations) measure the four Stokes parameters: I = total intensity, Q = linear polarization, U = orthogonal linear polarization, and V = circular polarization. From the combination of these parameters, it can be calculated the total linearly polarized intensity $P = (U^2 + Q^2)^{1/2}$ and the intrinsic position angle on the sky $\theta = 0.5$ arctan (U/Q) (apparent orientation of the projected E vector).

In theory the B vector is orthogonal to the E direction. In practice, however, the observed polarization can be highly compromised by Faraday rotation (rotation of the E field vector during the propagation inside the SNR and in the ISM). The angle of rotation is $\psi = \mathrm{RM}\lambda^2$, with RM, the rotation measure, defined as

$$\mathrm{RM(rad/m^2)} = 0.81 \int \mathrm{N(cm^{-3})B_{||}}(\mu\mathrm{G})\mathrm{dl\ (pc)}$$

where N is the thermal electron density, $B_{||}$ is the magnetic field component along the line of sight l, and the integral extends along the entire path. The sign of RM is determined by whether $B_{||}$ points toward or away from the observer. In general, observations at three or more radio wavelengths are necessary to measure the RM without ambiguity and determine the true position angles of the magnetic field lines.

At large spatial scale, it was proposed that the intrinsic orientation of the magnetic field in SNRs follows a typical pattern depending on their age, with the magnetic field in young SNRs predominantly radial, whereas for older remnants, the B vectors would be nearly tangential to the direction of the brighter shell emission. Polarization measurements carried out in 1987 by Milne over 27 SNRs seemed to confirm those early conclusions. Subsequent observations with improved instruments supported in general this picture (e.g., the SNR DA530, Landecker et al. 1999). Such distribution is generally explained with the argument that the tangentially ordered fields in old SNRs originate by compression of the interstellar field lines in radiative shocks with large shock compression ratios, while the radial orientation has been generally attributed to stretching of R-T instability fingers that occurs at the contact discontinuity, although in this last case the origin is still discussed.

An example of tangential B field along the bright rim is shown in Fig. 3 (*Left*) in the SNR CTB 1, while Fig. 3 (*Right*) shows the B field in SN1006 with a radial alignment near the forward shock. In addition, in this SNR, it can be noticed that the brightest NE and SW lobes have the lowest polarization fractions (indicating the presence of a disordered, turbulent magnetic field), while in the SE where the synchrotron emission is very weak, the polarization is high (ordered field).

Synchrotron theory predicts that the intrinsic degree of linear polarization is as high as 70 % for a source with $\alpha = 0.5$, but this high percentage is never attained in

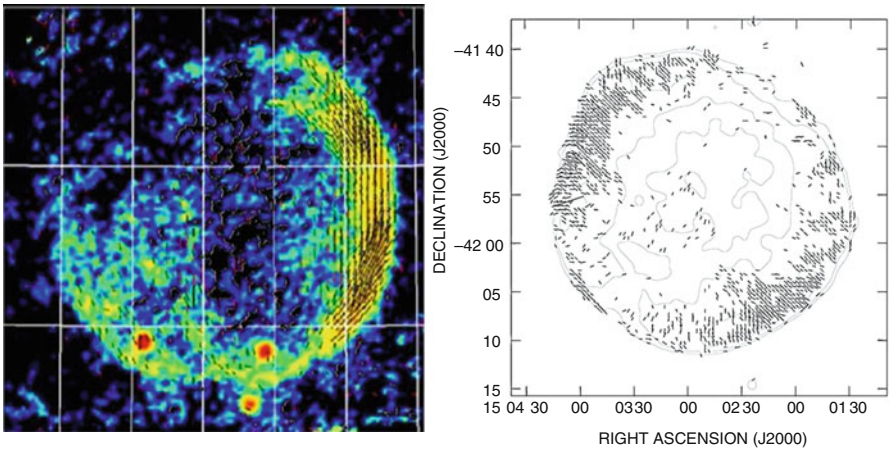

Fig. 3 *Left:* Radio polarization bars in B-field direction in the SNR CTB1 (Courtesy of W. Reich). *Right:* the same in SN1006 (From Reynoso et al. 2013)

practice. In some few exceptional cases, polarizations as high as 35 % to 60 % have been observed (e.g., in SN1006), but in general the polarization is found around 10 % to 15 %. This is possibly an indication that the magnetic fields are primarily disordered, probably tangled at small scales.

Polarization studies are complex in practice because, in addition to Faraday rotation, there are a number of effects that can modify or corrupt polarized signals in radio telescopes (e.g., instrumental polarization), involving several corrections to the data.

The estimate of the strength of magnetic fields is another very difficult task. One way relies on the assumption of equipartition between particle and magnetic energy, as will be described in the next section. A much more precise way to estimate the magnetic field strength is through Zeeman splitting in OH (1720 MHz) masers. Using this technique, magnetic fields in the range from ∼0.2 to ∼2.5 mG have been estimated for several galactic SNRs (see Brogan et al. 2013 and references therein). The drawback of this method is that it can be applied to scarcely a 10 % or less of the SNRs catalogued in our galaxy, that is, the SNRs that are interacting with molecular clouds, the necessary (but not sufficient) condition to stimulate OH (1720 MHz) maser emission.

1.5 The Energy Content in SNRs

If we assume that each electron only radiates at its critical frequency, we can obtain an expression for the electron energy content from synchrotron theory. This can be done by integrating over the electron spectrum between energies E_1 and E_2:

$$U_6 = \frac{LC_1^{1/2}}{C_3 B^{3/2}} \frac{(2-2\alpha)}{(1-2\alpha)} \frac{(v_2^{1/2-\alpha} - v_1^{1/2-\alpha})}{(v_2^{1-\alpha} - v_1^{1-\alpha})} (\text{if } \alpha \neq 0.5 \text{ or } 1)$$

where if evidence of cutoff is observed at one end or the other of the radio spectrum, the total electron energy is expressed in terms of the critical frequencies for the cutoff energies, ν_1 and ν_2, and the spectral index α. L is the total luminosity of the source estimated from the observed flux density assuming isotropic radiation ($L = 4\pi\, d^2\, S$, d being the distance to the source and S the flux density); B is the average strength of the magnetic field, and the constants C_1 and C_3 take the values 6.266×10^{18} and 2.368×10^{-3} in cgs units, respectively. The lower cutoff energy can be taken equal to the electron rest mass energy (if the electron is not relativistic, it does not produce synchrotron radiation). It is customarily assumed a lower cutoff frequency of 10^7 Hz. For the upper cutoff, a value derived from X-ray data can be used when it is possible. If there is no other indication, 10^{10} or 10^{11} Hz is adopted.

The energy of a source emitting synchrotron radiation is mostly contained in two forms: kinetic energy of the accelerated particles, U_{part}, and the energy stored in the magnetic field U_{mag} (thermal radiation is usually small compared to the formers, and gravitational energy is not considered as almost nothing is known about it). To

estimate the energy stored in particles, we have to take into account that in addition to electrons, there must be protons and other energetic baryons in the radiating source (though heavy particles emit negligible amounts of radiation because they are accelerated much less by the Lorentz force). Therefore, $U_{part} = \eta U_e$, where η is a factor that takes all other particles into account. From various methods, η has been estimated to be 50 (the value from cosmic rays near Earth) or 100 (from models applied to radio sources in our galaxy, e.g., Burbidge 1959). Fortunately, as shown below, this uncertainty does not have a strong effect on the fundamental conclusions. The energy stored in the magnetic field for a source of volume V is $U_{mag} = VB^2/8\pi$. Therefore

$$U_{tot} = U_{part} + U_{mag} = \eta ALB^{-3/2} + VB^2/8\pi$$

where A takes into account the constants C_1, C_3 and the shape factor in frequency. It is easily noticed that particle energy dominates for small field strengths and magnetic energy dominates for large fields. In consequence, the total energy has a minimum for a specific magnetic field intensity $B(U_{min}) = (6\pi aAL/V)^{2/7}$, for which $U_{part}/U_{mag} = 4/3$, very close to equipartition of energy between relativistic particles population and magnetic fields. If the magnetic field has exactly the intensity that minimizes the total energy, then

$$U_{min} = 0.5(\eta AL)^{4/7} V^{3/7}.$$

In this way, it is possible to obtain a lower limit of the energy requirements for a synchrotron source and provide an approximate estimate of the magnetic field intensity. However, it has to be noticed that in fact there is no physical justification for the energy components of a source are close to equipartition. Motions in the plasma may stretch and tangle the magnetic fields, while turbulent motions may also accelerate particles to high speeds, taking the plasma closer to equipartition, but these are only conjectures, and the real radio source can be far from energy equipartition. For the fundamental concepts of minimum energy calculations, see, for example, Pacholczyk (1970). Also Arbutina (2012) presents some improvements in the approximate calculations.

1.6 The Morphology of Radio SNRs and Its Physical Meaning

Now, after examining the origin of the radio emission from SNRs and the various mechanisms at play, the different morphologies observed in radio wavelengths can be analyzed and interpreted. The shape and brightness distribution in SNRs contain a significant amount of information that helps to constrain the physical characteristics of the progenitor star, the explosion mechanism, the evolutionary characteristics, and, sometimes, the consequences of interaction between expanding SNR and the surrounding interstellar medium (ISM).

Radio SNRs have been traditionally classified in three broad categories based on their appearance, namely, **shell type**, **composite**, and **filled center**. More recently, these categories have been complemented with a fourth one: **mixed morphology** (M-M). They represent different classes of objects within the family of SNRs.

1.6.1 Shell-Type SNRs

They are characterized by a limb-brightened shell or ring whose external edge normally marks the current location of the shock front, with a relatively hollow interior (except for projection effects of the front and/or rear parts of the emitting shell that visually seems to fill in the central parts in a two-dimensional image). The sharp radio edge (when it is well defined) usually coincide with the onset of the X-ray emission coming from the interior of the bubble. When the shape is clearly ring-like, the thickness of the annulus is approximately 10 % to 30 % of the shell radius. For this class of radio remnants, the particles responsible for the synchrotron radiation are believed to be accelerated at the shock front, and the magnetic field is the compressed interstellar field with possibly other mechanisms in action to augment it. In some cases, a faint, diffuse radio halo is observed upstream (i.e., in front of the sharp rim) with an intensity of about 10 % of that just inside the edge. This emission originates in relativistic electrons that have diffused upstream from the shock.

Young SNRs (ages of a few thousand years or younger) are more likely to retain the spherical symmetry, since the interaction with the inhomogeneous surrounding gas has not still affected them in a noticeable way. Usually the position of the shock front is marked by a steep increase in radio brightness, although the outer border of the shells does not have a unique characteristic pattern. Some radio remnants show a sharp limb-brightened border, at least in parts of the periphery, as in the case of the Tycho's SNR mostly along its western border (Fig. 4, *top left*), or in parts of the SN1006 SNR (Fig. 4, *top right*). In other cases, however, the outer boundary looks irregular and/or blurred like in the cases of the SNR Cas A (Fig. 4, *bottom left*) and Kepler's (Fig. 4, *bottom right*). In particular, in the case of Cas A, it can be noticed that the brightest radio emission occurs in a ring interior to the outermost border. In Kepler's SNR, the presence of a faint outer halo is observed to the south and other parts of the boundary. It has to be remarked that all the compared images have been obtained with very good angular resolution (between 1" and ∼5") and that Cas A, Kepler's, and Tycho's SNRs have comparable angular sizes (5', 3', and 8', respectively) and are located at roughly comparable distances (3.4, 3, and 2.4 kpc, respectively), indicating that the differences observed in the appearance have a real physical origin and are not a consequence of different quality of the observations. SN1006 is the more extended of the historical SNRs, with an angular diameter of 30', located at 2.2 kpc. In this case, the fact that the remnant is located very high above the galactic plane, expanding in a relatively low-density environment, has probably contributed to maintain the spherical symmetry.

The shell-type class comprises the largest number of catalogued SNRs in our galaxy. Over 70 % of the Milky Way SNRs have a shell-type morphology, although this group includes many objects where the observed shell is broken, incomplete,

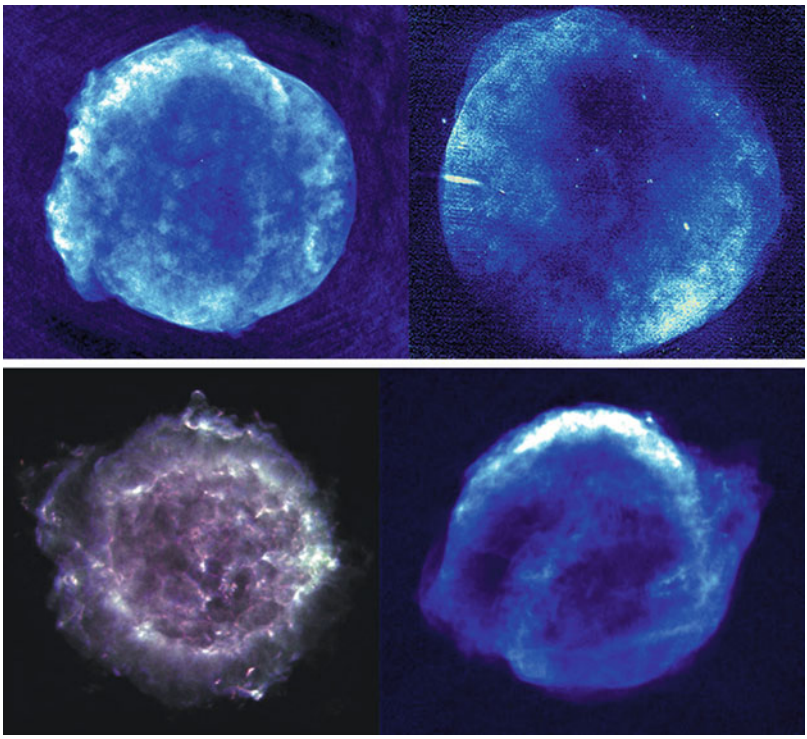

Fig. 4 *Top left:* Tycho's SNR observed at 1.4 GHz (beamsize 1".4) with the VLA (NRAO) from Reynoso et al. (1997). *Top right:* SN1006 observed at 1.5 GHz (beamsize 7".6 × 4".9) with the ATCA (Australia) and the VLA (NRAO) from Reynoso et al. (2013). *Bottom left:* the SNR Cas A in a composition of emissions at 1.4, 5.0, and 8.4 GHz (Image displayed with a beamsize of 2".5, courtesy of NRAO/AUI). *Bottom right:* Kepler's SNR at 5 GHz as observed with the VLA (NRAO) (beamsize 1") (Courtesy of T. Delaney, West Virginia Wesleyan College, USA) (See also DeLaney et al. 2002)

and sometimes amorphous or with curious shapes. Examples of these "atypical" SNRs classified as of shell-type class are shown in Fig. 5, including (*left*) the SNR W50, with the microquasar SS433 at its center, and the SNR G340.6+0.3 (*right*), where the elongated, helical shape remains unexplained.

The distribution of the surrounding gas, as well as the local orientation of the interstellar magnetic field, has also strong influence on the morphology of the radio remnants. Figure 6 (*Left*) illustrates a peculiar case of morphology determined by the inhomogeneous density distribution of the environmental gas. The SNR VRO 42.05.01 exploded in a warm, intermediate-density medium and later expanded in a hot, tenuous interstellar cavity re-energizing a section of it. SNRs with this kind of shape are usually labeled as "break-out" remnants. The SNR G18.8+0.3 (Fig. 6 *Right*), on its side, has encountered a dense environment in the side closer to the galactic plane, while at higher latitudes the SNR shock freely expands in a lower-density medium.

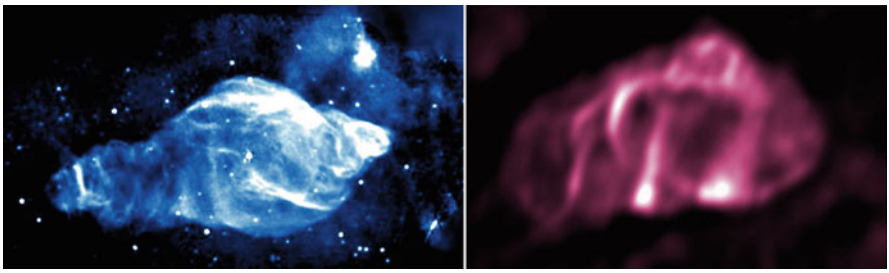

Fig. 5 *Left:* The SNR W50 with the X-ray binary SS433 at its center as observed at 1465 MHz with the VLA (NRAO), from Dubner et al. (1998). *Right:*The SNR G340.6+0.3 observed at 1425 MHz with the VLA (NRAO) from Dubner et al. (1996)

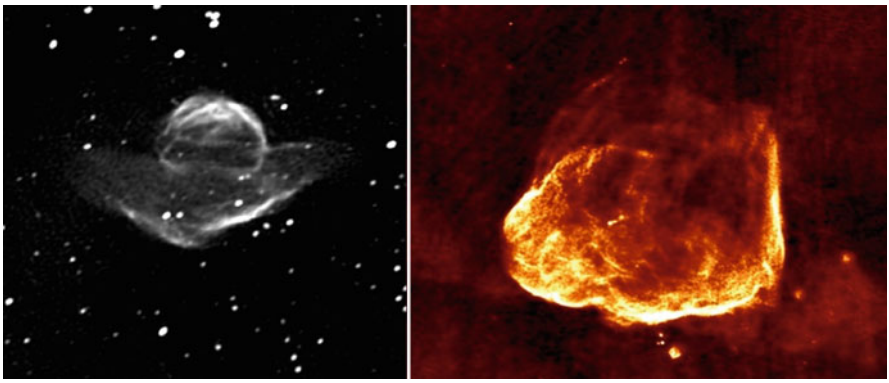

Fig. 6 *Left:* The SNR VRO 42.05.01 observed at 1.4 GHz with the DRAO (Canada) interferometer (From Pineault et al. 1987). *Right:* SNR G18.8+0.3 at 1.4 Gz (From the FIRST VLA Survey). In both cases, the morphology is the consequence of a large density contrast in the surrounding interstellar gas

Bilateral (also known as bipolar, axisymmetric or "barrel"-shaped) remnants constitute another morphological population within the shell-type SNRs. These are SNRs with a clear axis of symmetry and two bright limbs on either side. In most, but not all, of the bilateral SNRs, the symmetry axis is more or less parallel to the galactic plane. Different explanations have been proposed for this peculiar shape, either of extrinsic origin, like density stratification parallel to the galactic plane, preferred alignment of the magnetic field (which at least for low latitudes is well ordered and runs nearly parallel to the galactic plane), and/or quasi-perpendicular acceleration of electrons in the SN shock. Intrinsic models based on the existence of SN jets, explosions with bilateral geometry, etc. have also been considered. Examples of this class are SN1006 (Fig. 4 *upper right*) and G296.5+10.0 (two cases where the symmetry axis is perpendicular to the galactic plane). This class has been extensively investigated by Gaensler (1998), while West et al. (2015) and references therein discuss different alternative origins. However, it has to be noted

that some members of this group are not pure shell-type SNRs but may be related to the composite type that is discussed below.

1.6.2 Composite SNRs

They are characterized by the presence of a central nebula (usually bright) with the radio brightness peaking at the center, and surrounding this nebula is an external shell with physical properties similar to the previous case. For the central nebula, the origin of relativistic particles and magnetic fields is different from what was discussed until now. Both accelerated particles and magnetic fields are provided by a rapidly rotating neutron star (NS) created after the stellar core collapse. The NS loses energy with a rate $\dot{E} = I\Omega\dot{\Omega} = 4\pi^2 I\dot{P}/P^3$, where Ω is the angular frequency, P the rotational period, and I $\approx 10^{45}$ g/cm^2 the moment of inertia. This energy loss produces a wind of relativistic electrons and positrons, which terminates in a shock where electrons and positrons are accelerated to ultrarelativistic energies. These particles advect and diffuse away from the shock creating a nebula that emits synchrotron radiation, the so-called pulsar wind nebula (PWN). In some cases, PWNs have been observed from radio wavelengths to high-energy gamma-ray emission.

The radio PWN is characterized by a flat spectral index $0 \leq \alpha \leq 0.3$ and high linear polarization, while the surrounding shell has steeper spectrum α between approximately 0.4 and 0.7, as predicted from DSA. In some cases, the pulsar itself is not detected (as is the case much more often than not), but the mere existence of a synchrotron nebula indicates that an energetic pulsar must be located within. Pulsars may not be detected due to unfavorable beaming, insufficient sensitivity for very distant SNRs, significant scattering, dispersion along the line of sight, etc.

In summary, composite SNRs are those where two different origins for the synchrotron emission are at work simultaneously: shock acceleration and magnetic field compression in the shell created by the SN blast wave and wind of relativistic particles and Poynting flux from the spinning NS in the center. Figure 7 shows two composite SNRs of different appearance: the SNR W44 (*Left*), where the pulsar location is indicated by a white cross and the PWN is the small cometary-shaped nebula with the pulsar in its head, and the SNR G0.9 + 0.1 (*Right*) with a very structured central PWN surrounded by a faint circular radio shell.

1.6.3 Filled Center or Crab-Like (a.k.a. Plerions)

Sometimes the shell is not formed (e.g., if the ambient density is very low), or after thousands of years, the shell vanishes into the surrounding medium while the PWN survives, or the NS and its associated PWN move away (NSs are born with kick velocities of several hundreds of km/s) leaving behind the host SNR. In these cases, the naked PWN survives without a radio shell, constituting the third class of radio SNRs named "filled center" or "plerions." The prime example of this class is the Crab Nebula (Fig. 8) that emits synchrotron radiation across the whole electromagnetic spectrum. Despite several deep searches, no shell has been ever detected around Crab to remarkably low upper limits. As it is a young SNR, less than a thousand years old, it is highly unlikely that it has lost its shell because

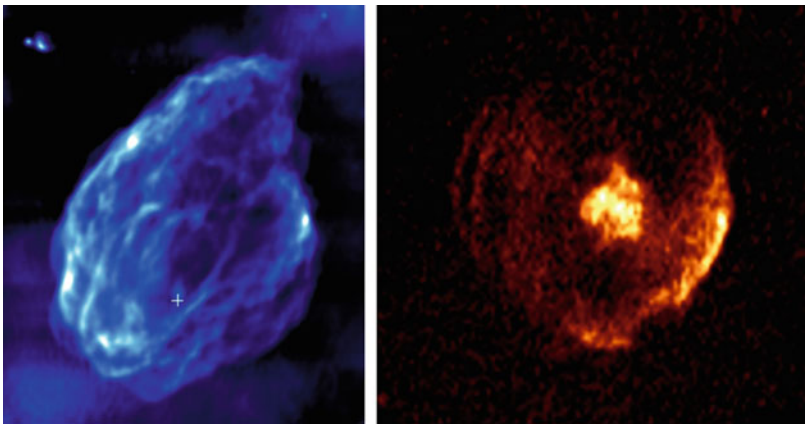

Fig. 7 *Left:* The SNR W44 as observed at 1.4 GHz with the VLA (NRAO) (From Giacani et al. 1997). The pulsar wind nebula is the small cometary-shaped feature observed in the southern half of the SNR, with the pulsar indicated by a white cross. *Right:* The SNR G0.9+0.1 as observed at 330 MHz with the VLA (NRAO) (From Nord et al. 2004), with a large and structured pulsar wind nebula in its center

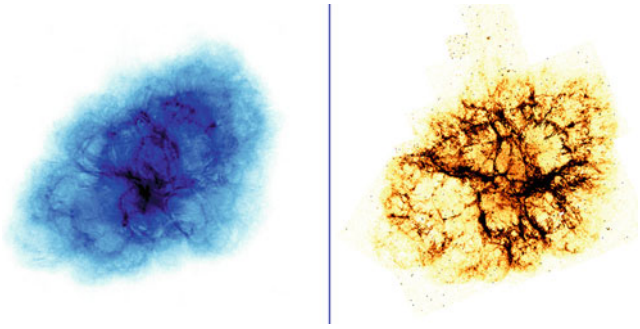

Fig. 8 *Left:* The Crab Nebula as observed at 3 GHz with the JVLA (NRAO) with an angular resolution better than 1" (From Dubner and Giacani 2015). *Right:* Optical image in the OIII line as observed with the Hubble Space Telescope (Image Credit: NASA, ESA, J. Hester, A. Loll). Some features are identical in both spectral regimes, while other differs

of aging; also the surroundings are not excessively evacuated (in comparison to other still detectable shells). It has been proposed that while the pulsar has released about 10^{50} ergs into the nebula, the SN explosion itself was under-energetic (merely few times 10^{49} ergs), i.e., a weak explosion but with a powerful pulsar. Only 3 % of the catalogued galactic SNRs belong to this class. Other examples are 3C58 (G130.7+3.1, with the pulsar J0205+6449 possibly associated) and MSH 15–57 (G328.4+0.2, with an as yet undetected pulsar).

1.6.4 Mixed Morphology (M-M)

These SNRs are "false" composites as they have a normal synchrotron expanding radio shell together with center-filled emission, but in this case, the central nebula, instead of radiating nonthermal synchrotron in radio or other wavelengths, emits thermal X-rays. The SNRs of this class, designated as such in 1998 by Rho and Petre, are found that in most cases are interacting with dense interstellar clouds. The majority of M-M SNRs is associated with gamma-ray sources, mostly of hadronic nature (when relativistic particles collide with dense ambient targets producing pions which decay into gamma ray). These sources have been modeled as remnants expanding in a cloudy environment where the centrally bright X-ray emission would come from small ISM cloudlets engulfed by the main shock front and heated up to X-ray-emitting temperatures (evaporated clouds). Other models propose that thermal conduction in the hot interior of the remnant prevents the formation of a vacant interior (see, e.g., White and Long 1991 and Cox et al. 1999). Examples of these remnants are W28, CTB1, 3C400.2, HB21, 3C397, etc.

In summary, theoretically only two types of SNRs would be expected: **pure shell type,** the remnant of the thermonuclear explosion of a white dwarf (SN Ia) that completely destroys a $\approx 1.4 M_{\odot}$ star in the explosion releasing $\approx 1.5 \times 10^{51}$ erg, in which case we should see the consequences of the expanding shock wave interacting with surrounding (circumstellar and/or interstellar) material, and **composite type** produced by a core-collapse explosion of a massive star, M $\approx$ 3 to 20 $M_{\odot}$, that creates a rotating neutron star and releases $\approx 10^{49}$ to 2×10^{51} ergs into the ISM, in which case a central PWN surrounded by a shell should be the detectable remains. Nature, however, is much more complicated, and the existence of naked PWN, incomplete arcs, amorphous nebulae, or twisted features is not a consequence of insufficient quality of observations, but on the contrary, the better the observations are, based on data from highly sensitive and spatially resolving radio telescopes, the greater variety of shapes is found among SNRs, reflecting different properties of the progenitor star and of explosion mechanisms, the properties of the ambient magnetic field, and the matter distribution in the circumstellar and interstellar medium. Disentangling the different causes is a complex task that remains a central question.

1.7 Can the SN Type Be Inferred from the Characteristics of the Radio SNRs?

This has been a challenging question for decades. Several attempts have been made to infer the type of supernova on the basis of the observed remnants. This is hardly possible in the radio range. In the first place, radio SNRs are blind to the chemical composition of the pre-supernova. Besides, the morphological criteria (circularity and mirror symmetry of the SNRs) that in X-rays and IR serve to discriminate the type of SN do not work for radio SNRs. The "circularity" criterion is clearly useless for radio remnants where, for example, Cas A (core collapse) and Tycho's

SNR (Type Ia) have similar circular morphology. Also, two examples of "mirror-symmetric" sources, SN 1006 and G296.5+10.0, come from different explosion types (Ia and core collapse, respectively).

One important reason that complicates the connection of a radio SNR with its precursor is that the details of the radio emission depend on the complex interaction between the shock front and the ejecta, circumstellar, and interstellar matter, rather than on the precursor star. The rapid expansion of the blast wave can soon mask the precursor information in the radio emission, since once the shock front sweeps up a certain amount of ambient gas, the radio synchrotron emission ignores the explosion properties, and it is mostly conditioned by the characteristics of surrounding medium, hydrodynamic instabilities in the flow, turbulence behind the shock, effects of magnetic fields, etc.

In a few cases, the traces left by mass loss episodes that the star suffered prior to its explosion can provide some clue to identify the class of supernova. The presence of an NS inside the remnant and/or the existence of the PWN is an unquestionable evidence of a core-collapse event, but the absence of it does not prove anything because pulsars have high kick velocities and can rapidly be outside the SNR, far from the explosion site. An indirect indicator of core-collapse SN would be the fact of finding the SNR very close to, or immersed in, a molecular cloud that might have been the birthplace of a massive star that ended its life as SN Ib, Ic, or II. In summary, the radio morphology alone is not a useful tool to distinguish between different types of SNe.

2 Conclusions

Since the first detection in radio waves of the SNR Cas A by Ryle and Smith far back in 1948, to the present, great advances in the knowledge of the properties of SNRs have been achieved, thanks to the existing body of radio studies. Radio observations allow us to trace the current location of the expanding shock front, to identify sites of particle acceleration, to infer orientation and degree of order of compressed magnetic fields, and to investigate the coupling between the magnetized relativistic wind of the central neutron star and the surrounding plasma. Also, radio observations are a powerful tool to discover new SNRs in our galaxy as well as in neighboring galaxies.

At the present time, there are 294 firmly classified SNRs in our galaxy, of which 280 are radio sources. This number, however, is barely one third of the number of SNRs statistically predicted on the basis of OB stars count, pulsar birth rates, SN rates in other local group galaxies, and predicted lifetime of radio synchrotron-emitting sources in the sky. Such deficit is generally attributed to selection effects when old, faint, large remnants, as well as young, small sources, remain below the threshold in sensitivity and/or spatial resolution of the galactic surveys performed up to now. The prime radio telescopes in operation, commissioning, or construction phase, like the Karl G. Jansky Very Large Array (JVLA, the upgraded version of the VLA) in the USA, the Atacama Large Millimeter Array (ALMA) in Chile,

the Australian Square Kilometre Array Pathfinder (ASKAP) in Australia, the MeerKAT (the precursor of the South African part of the Square Kilometre Array (SKA)), the Long Wavelength Array (LWA) in the USA, the Five-Hundred-Meter Aperture Spherical Telescope (FAST) in China, the SKA in South Africa-Australia-New Zealand, etc., surely will bring important advances not only allowing us to underscore missing remnants but also bringing new insights on the properties of the radio SNRs through very high-dynamic range images that help to reveal extremely faint emission, the detailed study of small-scale variations of the magnetic field, and spectral features originated in the interactions between the SNR shock and dense clumps in the surrounding gas.

3 Cross-References

- ▸ Dynamical Evolution and Radiative Processes of Supernova Remnants
- ▸ Pulsar Wind Nebulae
- ▸ Supernova Remnants as Clues to Their Progenitors
- ▸ The Supernova – Supernova Remnant Connection

Acknowledgements I am grateful for the hospitality of the JVLA (NRAO) P. Domenici Science Operations Center in Socorro (NM, USA), where part of this work was carried out. I thank CONICET (Argentina) for the support through the Grant PIP 0736/11 and to ANPCyT (Argentina) through the Grant PICT 0571/11. I have used images provided by T. Delaney, E. Reynoso, and W. Reich with permission of the authors, whom I thank. I am a member of the "Carrera del Investigador Científico" from CONICET, Argentina.

References

Alfvén, H., Herlofson, N. (1950), Cosmic Radiation and Radio Stars, Ph Rv, 78, 616

Arbutina B, Urošević D, Andjelić MM, Pavlović MZ, Vukotić B (2012) Modified Equipartition Calculation for Supernova Remnants. ApJ 746:79

Bell AR, Schure KM, RevilleB (2011) Cosmic ray acceleration at oblique shocks. MNRAS 418:1208

Blandford R, Eichler D (1987) Particle acceleration at astrophysical shocks: a theory of cosmic ray origin. Phys Rep 154:1

Brogan CL, Goss WM, Hunter TR, Richards AM, Chandler C, Lazendic JS, Koo B-C, Hoffman IM, Claussen MJ (2013) OH (1720 MHz) Masers: a multiwavelength study of the interaction between the W51C supernova remnant and the W51B star forming region. ApJ 771:91

Burbidge GR (1959) Estimates of the total energy in particles and magnetic field in the non-thermal radio sources. ApJ 129:849

Castelletti G, Dubner G, Clarke T, Kassim N (2011) High-resolution radio study of SNR IC 443 at low radio frequencies. A&A 534:21

Cox DP, Shelton RL, Maciejewski W, Smith RK, Plewa T, Pawl A, Różyczka M (1999) Modeling W44 as a supernova remnant in a density gradient with a partially formed dense shell and thermal conduction in the hot interior. I. The analytical model. ApJ 524:179

DeLaney T, Koralesky B, Rudnick L, Dickel JR (2002) Radio spectral index variations and physical conditions in Kepler's supernova remnant. ApJ 580:914

Dubner G, Giacani E, Goss WM, Moffett D, Holdaway M (1996) VLA observations of nine galactic supernova remnants. AJ 111:1304
Dubner G, Holdaway M, Goss WM, Mirabel F (1998) A high-resolution radio study of the W50-SS 433 system and the surrounding medium. AJ 116:1842
Dubner G, Giacani E (2015) Radio emission from supernova remnants. Astron Astrophys Rev 23:3
Gaensler B (1998) The nature of bilateral supernova remnants. ApJ 493:781
Giacani E, Dubner G, Kassim N, Frail D, Goss WM, Winkler PF, Williams BF (1997) New radio and optical study of the supernova remnant W44. AJ 113:1379
Green D (2014) A catalogue of 294 galactic supernova remnants. Bull Ast Soc India 42:47; VizieR Online Data Catalog: VII/272. https://www.mrao.cam.ac.uk/surveys/snrs/
Jones TW (2011) Particle acceleration at shocks: insights from supernova remnant shocks. J Astrophys Astron 32:427
Landecker TL, Routledge D, Reynolds SP, Smegal RJ, Borkowski KJ, Seward FD (1999) DA 530: a supernova remnant in a stellar wind bubble. ApJ 527:866
Malkov MA, O'C Drury L (2001) Nonlinear theory of diffusive acceleration of particles by shock waves. Rep Prog Phys 64:429
Nord ME, Lazio TJ, Kassim N, Hyman S, LaRosa T, Brogan C, Duric N (2004) High-resolution, wide-field imaging of the galactic center region at 330 MHz. AJ 128:1646
Pacholczyk AG (1970) Radio astrophysics. Nonthermal processes in galactic and extragalactic sources. Freeman, San Francisco
Pineault S, Landecker T, Routledge D (1987) VRO 42.05.01 – a supernova remnant reenergizing an interstellar cavity. ApJ 315:580
Reynolds SP (2008) Supernova remnants at high energy. ARA&A 46:89
Reynolds SP (2011) Particle acceleration in supernova-remnant shocks. Ap&SS 336:257
Reynolds SP, Gaensler BM, Bocchino F (2012) Magnetic fields in supernova remnants and pulsar-wind nebulae. Space Sci Rev 166:231
Reynoso E, Moffett D, Goss WM, Dubner G, Dickel J, Reynolds S, Giacani E (1997) A VLA study of the expansion of Tycho's supernova remnant. ApJ 491:816
Reynoso E, Hughes JP, Moffett DA (2013) On the radio polarization signature of efficient and inefficient particle acceleration in supernova remnant SN 1006. AJ 145:104
Schure KM, Bell AR, O'C Drury L, Bykov AM (2012) Diffusive shock acceleration and magnetic field amplification. Space Sci Rev 173:491
Uroševi'c D (2014) On the radio spectra of supernova remnants. Ap&SS 354:541
West JL, Safi-Harb S, Jaffe T, Kothes R, Landecker TL, Foster T (2015, in press) The connection between supernova remnants and the galactic magnetic field: a global radio study of the axisymmetric sample. A&A. (arXiv:1510.08536)
West JL, Safi-Harb S, Jaffe T, Kothes R, Landecker TL, Foster T (2016) The connection between supernova remnants and the galactic magnetic field: a global radio study of the axisymmetric sample, A&A, 587, 148
White RL, Long KS (1991) Supernova remnant evolution in an interstellar medium with evaporating clouds. ApJ 373:543
Whiteoak JB, Gardner FF (1968) A supernova remnant in centaurus. ApJ 154:807